

# Dependency of cardiac rubidium-82 imaging quantitative measures on age, gender, vascular territory, and software in a cardiovascular normal population

John J. Sunderland, PhD,<sup>a</sup> Xiao-Bo Pan, PhD,<sup>b</sup> Jerome Declerck, PhD,<sup>b</sup> and Yusuf Menda, MD<sup>a</sup>

<sup>a</sup> Department of Radiology, University of Iowa, Iowa City, IA

<sup>b</sup> Siemens Molecular Imaging, Oxford, UK

Received Apr 7, 2014; accepted May 13, 2014

doi:10.1007/s12350-014-9920-6

**Objectives.** Recent technological improvements to PET imaging equipment combined with the availability of software optimized to calculate regional myocardial blood flow (MBF) and myocardial flow reserve (MFR) create a paradigm shifting opportunity to provide new clinically relevant quantitative information to cardiologists. However, clinical interpretation of the MBF and MFR is entirely dependent upon knowledge of MBF and MFR values in normal populations and subpopulations. This work reports Rb-82-based MBF and MFR measurements for a series of 49 verified cardiovascularly normal subjects as a preliminary baseline for future clinical studies.

**Methods.** Forty-nine subjects (24F/25M, ages 41-69) with low probability for coronary artery disease and with normal exercise stress test were included. These subjects underwent rest/dipyridamole stress Rb-82 myocardial perfusion imaging using standard clinical techniques (40 mCi injection, 6-minute acquisition) using a Siemens Biograph 40 PET/CT scanner with high count rate detector option. List mode data was rehistogrammed into 26 dynamic frames (12 × 5 seconds, 6 × 10 seconds, 4 × 20 seconds, 4 × 40 seconds). Cardiac images were processed, and MBF and MFR calculated using Siemens syngo MBF, PMOD, and FlowQuant software using a single compartment Rb-82 model.

**Results.** Global myocardial blood flow under pharmacological stress for the 24 females as measured by PMOD, syngo MBF, and FlowQuant were  $3.10 \pm 0.72$ ,  $2.80 \pm 0.66$ , and  $2.60 \pm 0.63$  mL·minute<sup>-1</sup>·g<sup>-1</sup>, and for the 25 males was  $2.60 \pm 0.84$ ,  $2.33 \pm 0.75$ ,  $2.15 \pm 0.62$  mL·minute<sup>-1</sup>·g<sup>-1</sup>, respectively. Rest flows for PMOD, syngo MBF, and FlowQuant averaged  $1.32 \pm 0.42$ ,  $1.20 \pm 0.33$ , and  $1.06 \pm 0.38$  mL·minute<sup>-1</sup>·g<sup>-1</sup> for the female subjects, and  $1.12 \pm 0.29$ ,  $0.90 \pm 0.26$ , and  $0.85 \pm 0.24$  mL·minute<sup>-1</sup>·g<sup>-1</sup> for the males. Myocardial flow reserves for PMOD, syngo MBF, and FlowQuant for the female normals were calculated to be  $2.50 \pm 0.80$ ,  $2.53 \pm 0.67$ ,  $2.71 \pm 0.90$ , and  $2.50 \pm 1.19$ ,  $2.85 \pm 1.19$ ,  $2.94 \pm 1.31$  mL·minute<sup>-1</sup>·g<sup>-1</sup> for males.

**Conclusion.** Quantitative normal MBF and MFR values averaged for age and sex have been compiled for three commercial pharmacokinetic software packages. The current collection of data consisting of 49 subjects resulted in several statistically significant conclusions that support the need for a software specific, age, and sex-matched database to aid in interpretation of quantitative clinical myocardial perfusion studies. (J Nucl Cardiol 2015;22:72-84.)

**Key Words:** Myocardial perfusion imaging; PET • myocardial flow reserve • coronary blood flow • Rb-82

---

**See related editorial, pp. 85–88**

---

## BACKGROUND

Absolute quantitative myocardial perfusion measurement is one of the earliest applications of quantitative clinical positron emission tomography (PET), as well as one of the most enduring.<sup>1–7</sup> Work with [<sup>13</sup>N]ammonia, [<sup>15</sup>O]H<sub>2</sub>O, and the potassium analog <sup>82</sup>Rb have all been used to varying degrees over the previous three decades, and numerous researchers have developed and reported upon quantitative approaches to estimating regional myocardial perfusion with these radiopharmaceuticals. [<sup>15</sup>O]H<sub>2</sub>O is widely regarded as the gold standard because of its linear uptake behavior over the entirety of the clinical perfusion range. [<sup>13</sup>N]ammonia and <sup>82</sup>Rb have well-studied flow-dependent extractions that make their performance nonlinear under high/hyperemic flow conditions and require an ad hoc flow-dependent extraction component to be applied to the model in order to accurately quantitate flow into the higher physiologic range. However, this nonlinear behavior is now well characterized and can and has been incorporated routinely into current quantitative imaging approaches.<sup>8</sup>

Myocardial blood flow measurements with normal and diseased populations have been investigated extensively over the past 30 years with these three tracers. These studies include (1) validation studies with microspheres or angiography,<sup>2,9,10</sup> (2) test/retest (usually with [<sup>15</sup>O]H<sub>2</sub>O or more recently Rb-82) to assess the reproducibility of PET-based myocardial blood flow measurements,<sup>11–14</sup> (3) comparison studies measuring different performances between PET tracers,<sup>11,15,16</sup> (4) quantitation of the hyperemic impact of pharmacologic stressing agents, including MFR,<sup>5,12,14,17–19</sup> and most recently (5) comparison of software performance.<sup>20,21</sup> In the course of these studies, several have reported MBF from various tracers in normal populations. Many of the reported measurements of normal flows were performed on previous generation scanners (prior to 2000) and with homegrown software.<sup>4,12,18,19</sup>

Despite this robust academic work in this area over several decades, only recently has routine quantitative assessment of myocardial perfusion for clinical purposes been aggressively pursued by the nuclear cardiology field at large. It is occurring now due to the confluence of several commercial and technological hurdles that have been recently cleared including development of high count rate 3D PET scanner detector technologies, prompt gamma corrections to compensate for the

additional 776 keV gamma associated with 13% of Rb-82 decays,<sup>22,23</sup> and high speed image reconstructions necessary for the real-time reconstruction of dynamic cardiac image data. Last, there is accumulating evidence in the literature supporting the prognostic predictive value of quantitative MBF and MFR.<sup>24–27</sup>

Quantitative perfusion imaging requires accurate measurement of the input function (blood concentration) of the radiopharmaceutical, the regional pixelwise concentration measurement of the radiotracer in the myocardium, and software that combines these two pieces of information within the context of a well-understood mathematical pharmacokinetic model. Only if all these pieces are in place can an accurate estimation of quantitative regional perfusion (mL·minute<sup>-1</sup>·g<sup>-1</sup>) be generated. The final piece enabling more global application of clinical quantitative myocardial perfusion is the recent development and availability of commercially available user-friendly pharmacokinetic software capable of making these regional myocardial perfusion and myocardial flow reserve estimates. At present there are at least ten available software packages that provide quantitation of MBF with PET; their general capabilities and approval statuses were recently reviewed by Saraste.<sup>28</sup>

This work reports on quantitative rest and stress (dipyridamole) myocardial imaging of 49 prospectively normal subjects ages 40–69, and the quantitative normal ranges of rest and stress MBF and MFR reported by myocardial segment. MBF and MFR estimates were made using three different commercially available software packages to assess software specific bias. Finally, the data was compiled into an age and sex-matched normal myocardial perfusion database against which to compare individual absolutely quantitative (mL·minute<sup>-1</sup>·g<sup>-1</sup>) patient perfusion images to make optimal clinical use of these new quantitative imaging capabilities.

## METHODS

### Study Population

Forty-nine subjects with a prospectively low-likelihood of coronary disease between the ages of 40–69 were recruited for participation in the study. The study protocol was approved by the local University of Iowa IRB and Medical Radiation Protection Committee and conforms to the principles outlined in the Declaration of Helsinki. All subjects agreed to informed consent prior to initiation of the study. Each subject completed a normal exercise ECG with no induced changes and had no major risk factors for CAD or a history of cardiac events. All subjects achieved the benchmark 85% of age predicted maximum heart-rate (99% ± 7%). MET levels were measured in all cases (all above 10 METS except two of the older patients who were slightly below) with double products >25,000 in all cases except two that were both >22,000).

Specific exclusion criteria included patients with a history of prior myocardial infarction, diagnosis of coronary artery disease (CAD) based on abnormal angiogram, patients with insulin-dependent diabetes, and any conditions for which dipyridamole would be contraindicated. This resulted in a patient population with a <5% pre-test likelihood of CAD based upon sequential Bayesian analysis of age, sex, asymptomatic presentation, and normal ECG (no S-T depression).<sup>29</sup> Five potential low-risk subjects were excluded from proceeding to the PET scan portion of the study because of either abnormal ECG or inability to meet exercise criteria. All subjects underwent Rb-82 PET/CT myocardial perfusion studies at the University of Iowa for both standard clinical, and fully quantitative perfusion assessment. Post-test exclusion criteria included an abnormal clinical interpretation of Rb-82 scan or any induced changes on the ECG from pharmacologic stress. One subject who received the Rb-82 PET/CT myocardial perfusion was subsequently excluded because the clinical scan was read as abnormal. Specifically, the subject population consisted of 10 subjects age 40-49 (5M/5F), 20 subjects aged 50-59 (10M/9F), and 20 subjects aged 60-69 (10M/10F). Stress data from a 52-year-old female was corrupted and therefore omitted from the stress and MFR analysis, but was included in the rest analysis resulting in 50 subjects for the rest data.

### **Rb-82 Image Acquisition and Reconstruction**

All rest and pharmacological stress Rb-82 PET/CT perfusion scans were performed on a Siemens Biograph 40 TruePoint PET/CT scanner with HIREZ and high count rate detectors. Subjects were instructed to strictly avoid all caffeine containing products (explicitly including coffee, tea, and chocolate) for 12 h prior to their scheduled imaging procedure. All subjects were fitted to 12-lead ECG, pulse oximeter, and blood pressure monitor.

Since accurate attenuation correction is essential for quantitation, two very low dose attenuation CT scans are performed, each, for the rest and stress Rb-82 scans as described below. The best fit attenuation CT was chosen to apply to the emission data.

Following patient positioning on the scanner bed, the first low dose CT (11 mAs, 120 keV, 2.7 seconds) was taken at end-expiration. Immediately following the CT, Rb-82 was infused for the resting study (99 mL elution volume, 25 mL patient volume, 1.1-1.5 GBq patient dose, and 37 MBq-second<sup>-1</sup> threshold rate, 50 mL-minute<sup>-1</sup> infusion rate). At the end of rubidium infusion, a 20 mL saline flush was performed at approximately the same infusion rate used with rubidium. All infusions were necessarily performed using the infusion sets specified by the generator vendor to assure quantitatively accurate tracer administration. The 6-minute list mode PET acquisition commenced precisely concomitant with the Rb-82 infusion initiation.

Following immediately after the conclusion of the rest rubidium acquisition, the second attenuation CT scan was performed at shallow breathing. The two reconstructed CT scans were overlaid on the emission data, and the CT that most accurately corresponds spatially to the emission data was

chosen for application for final reconstructions. If necessary, the best match CT was manually re-aligned with PET emission data by an experienced technologist for optimal matching.

For the pharmacologic stress portion of the imaging study, dipyridamole was administered (5 mL-minute<sup>-1</sup>) over 7 minutes via infusion pump. Three minutes after completion of administration of dipyridamole, infusion of Rb-82 began simultaneous with the 6-minute list mode acquisition. Immediately following the Rb-82 acquisition the first attenuation CT for stress images (3rd overall) was acquired end-expiration, followed by a second attenuation CT scan for stress (4th overall) at shallow breathing. Aminophylline, 125 mg was then administered to reverse any side effects from the dipyridamole. The best match CT was manually aligned with PET emission data by an experienced technologist if such manipulation was deemed necessary.

List mode data was rehistogrammed into 26 dynamic frames (12 × 5 seconds, 6 × 10 seconds, 4 × 20 seconds, 4 × 40 seconds) and reconstructed using standard clinical 3D OSEM reconstruction with 2 iterations, 21 subsets, and a 5 mm Gaussian smoothing filter onto a 168 × 168 matrix (2.7 × 2.7 pixel size, 2.0-mm slice thickness) using the best fit CT (repositioned, if necessary) for each PET acquisition. All data was corrected for attenuation, scatter (with prompt gamma correction), dead time, decay, and randoms (delayed). The PET/CT scanner, equipped with high count rate detectors, was previously tested for linearity up to activity levels and concentrations higher than those achieved in the current study.

### **Pharmacokinetic Modeling and MBF Calculation**

The resulting dynamic image dataset was processed using three different commercially available pharmacokinetic software packages: syngo MBF (Siemens Medical Solutions, Version VB10), PMOD (PMOD-PMOD Technologies, Switzerland Version 3.2), and FlowQuant (Ottawa Heart Institute, Ottawa Canada, Version 2.2). Of the three, only syngo MBF has 510(k) clearance for clinical use. MBF and MFR were calculated using a standard single compartment Rb-82 model. Options for use of a more complex 2-tissue compartment model were available for PMOD and FlowQuant, but not for syngo MBF. The single tissue compartment model was ultimately chosen for analysis for two reasons, first to enable direct comparisons between all three software platforms, and second because most recent published work uses this model. To the extent possible, modeling options were chosen in each respective software package to maximally harmonize the modeling approach to achieve most comparable results. Several publications in the literature discuss the relevant details of the modeling approaches for each software packages.<sup>7,13,16,20,30,31</sup>

All three software packages are largely automated, with optional operator intervention in the initial myocardium identification and reorientation steps. With all software packages the operator had the option to validate, or manually modify the reorientation before moving on to the model-fitting portion of the quantitation. An experienced operator on an

as-needed basis exercised this option. For consistency-sake, the software algorithm result was used unaltered if it generated reasonable and meaningful identification of the myocardium and blood pool and generated a meaningful reorientation to the primary left ventricular axis. If the algorithm failed because of physiological Rb-82 uptake outside of the myocardium (the most frequent reason in this population), the image data was cropped to exclude the confounding activity, and the myocardium identification and reorientation software was re-run. All three software packages have the inherent capability to implement motion correction to account for small patient motion during the scan and was enabled in all cases.

The arterial input function was collected from a volume of interest (VOI) automatically generated by the respective software packages. For input function measurements, syngo MBF uses a region at the base of the left ventricle, while PMOD uses a region in the center of the LV and the FlowQuant input function implementation allows a user configurable VOI. In all cases, the arterial input function VOI is positioned far enough away from the myocardium so as to avoid the need for a tissue spillover correction. Each of the software packages provided the capability to visualize the input function and tissue activity curves, and these were manually checked to assure that peak shapes and curve magnitudes were within reasonable ranges before calculations were finalized. Since the location of the myocardium and blood pool was previously visually confirmed, checking the curves was primarily to assure that the proper timing of infusion and imaging occurred.

The time-tissue activity curve is corrected for blood pool spillover from the left ventricle, with no spillover correction generated from the right ventricle. The time activity curve used in the fitting is derived from mixing LV blood component and tissue component: the mixing parameter is computed as part of the fitting process for all three software packages.  $K_1$  and  $k_2$  values are fit to approximately 400-500 pixels representing the myocardium in all software packages and visually displayed as quantitative bulls eye parametric flow and MFR maps at this resolution. For purposes of this summary analysis, the MBF are averaged within specific regions of interest (vascular territories or AHA 17 segments).

As a PET flow tracer, Rb-82 exhibits a well-characterized flow-dependent extraction at higher physiological flows that limits the ability to calculate myocardial blood flow directly from  $K_1$ , and requires an additional look-up table step to generate final flow values. All software packages use algorithms that reference the flow extraction curve reported by Lortie et al, but implementations are not identical. Modeling details, operational approaches, and assumptions specific to each of the software packages are presented in several publications.<sup>16,32</sup>

## Statistical Analysis

To assess software differences, quantitative flows calculated by cardiac segment were categorized by sex and age groups (40-49, n = 10, 5M/5F; 50-59, n = 19, 10M/9F; 60-69, n = 20, 10M/10F). Although the quantitative myocardial

blood flow estimates from each of the software packages generated results relatively consistent with one another (Figure 1, top two plots), they varied with a measureable and often statistically significant bias between them, with specific results detailed below. Because of these differences, summary blood flow data is reported specific to the software that generated the data, rather than in aggregate. In all cases a simple two-sided *t* test was employed when comparing two populations, except in the case of measuring differences in MBF between the sexes. In that case, consistent evidence exists suggesting higher blood flows for females than males, so a single-sided *t* test was used in that circumstance. Continuous variables are expressed as mean  $\pm$  1 standard deviation.

## RESULTS

### Software Comparison Results

A subject-by-subject rest and stress quantitative global myocardial flow comparison is shown in Figure 1A, B. From the plots, it appears that the flow calculations for both rest and pharmacologic stress correlate well, although systematic bias with PMOD > syngo MBF > FlowQuant is apparent. PMOD had a mean positive bias of 23% relative to FlowQuant results and a 13% positive bias when compared with syngo MBF. Statistically the PMOD generated significantly higher MBF values at the .05 level vs FlowQuant for male and female cohorts under both rest and stress conditions, and at the .01 level when all subjects were combined. Statistically significant differences between PMOD and syngo MBF were less compelling, with *P* values at the .1 level for all subjects combined under both rest and stress conditions (*P* = .074 for stress data, and *P* = .017 for rest data). syngo MBF had a 9% mean positive bias vs FlowQuant, although it did not reach statistical significance. Software generated MBF statistical comparisons are summarized in Figure 2. Software comparisons are also presented in a series of Bland-Altman plots in Figures 3 and 4 associated, respectively, with the rest and stress flows calculated by each of the programs.

No significant difference, or even reliable trend, was observed between software packages and their respective MFR data (Figure 1C). It is likely that the systematic biases for myocardial blood flow measurement of the software were approximately linear with flow, so bias canceled out in MFR ratio calculation.

### Results by Sex, Age, and Myocardial Segment

Quantitative myocardial blood flow and myocardial flow reserve calculation results for all three software packages, broken down by age, sex, and vascular territory are tabulated in Table 1. Summarized values with all ages combined are summarized in Table 2.

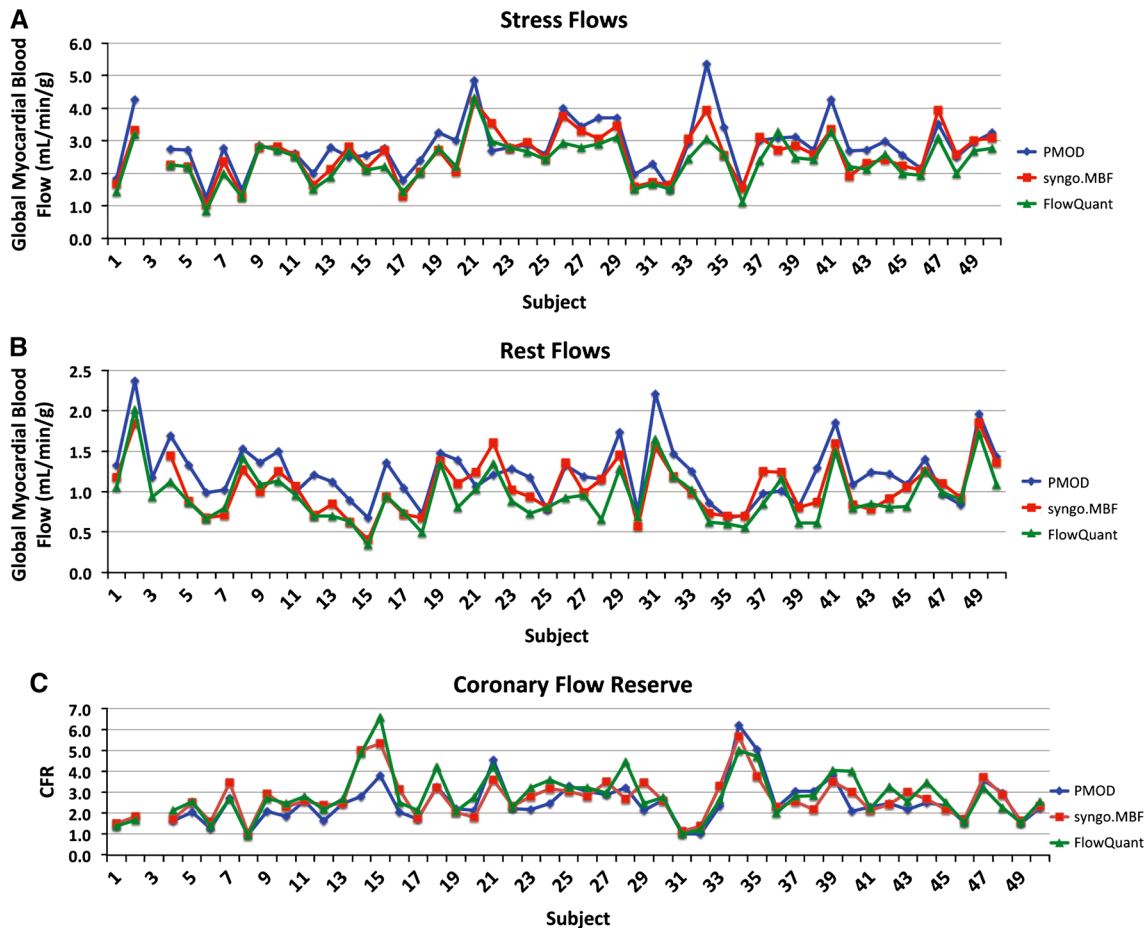


**Figure 1.** Subject by subject (A) rest and (B) stress MBF and (C) MFR comparisons for PMOD, syngo MBF, and FlowQuant for the 50 normal subjects studied. There was, in general, good MBF and MFR correspondence between software packages, however, small systematic biases between MBF values from the different software was observed and is apparent in both rest and stress measurements. Subject 3 stress data was compromised, and so stress and MFR data are necessarily omitted from the plot.

In graphical data presentation below, representative results from the various software investigated are presented to illustrate trends. In general trends by age, sex, and myocardial segment were reproduced across the software packages.

**Results by Sex.** Female myocardial blood flow values were, on average, approximately 20% higher than male myocardial blood flow values, both globally and per vascular territory. This trend was consistent across software packages and was apparent under both stress and rest conditions. Sample data from syngo MBF is shown in Figure 5, and demonstrates statistically significant differences at the .05 level for all vascular territories except the LAD (which was significant at the .10 level). Myocardial flow reserve did not show an obvious differentiation by sex. The data illustrates a weak tendency for

males having a slightly higher mean MFR than females, but that difference did not approach statistical significance.

**Results by Age.** Myocardial blood flow was calculated globally and for each cardiac segment on all three software platforms with sample results from syngo MBF in Figure 6. Trends for decreasing global MBF with age was observed for subjects between the ages of 40-69 for both males and females, and in all cardiac territories. This result is generally consistent with the published normal data, although this study did not accrue subjects younger than 40.

MFR measurements showed a very weak, non-significant positive trend with age. This tendency was evident with the other two software packages. This result runs counter to other literature reports<sup>18,19</sup> that suggested an opposite trend.

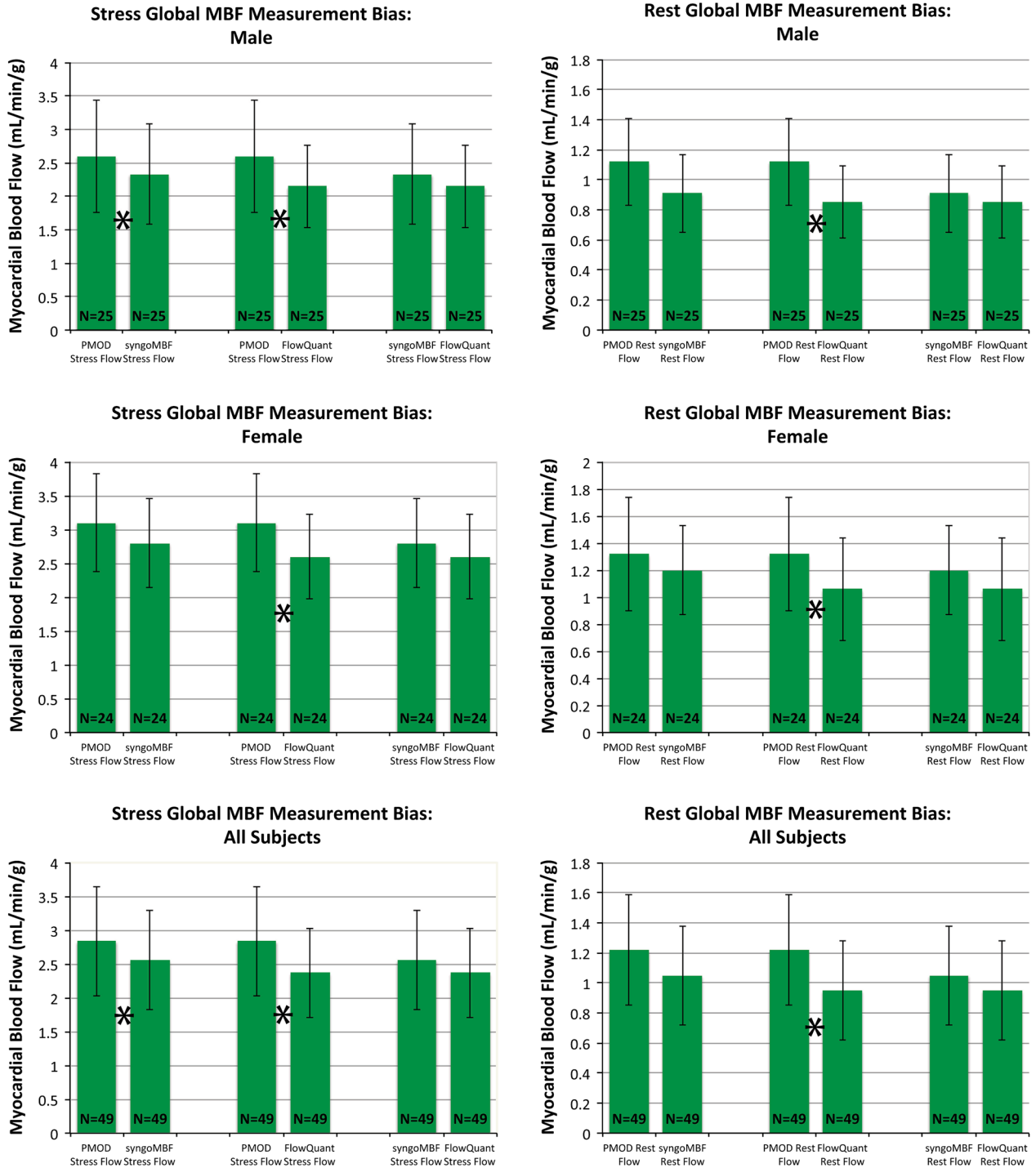


**Figure 2.** Two sided *t* test results illustrating systematic differences in myocardial blood flow measurements for the three software packages. In all cases illustrated above PMOD myocardial blood flow means were statistically higher (\*) than the corresponding FlowQuant values at the *P* = .05 significance level. 25 normal male subjects and 25 normal female subjects made up the illustrated populations.

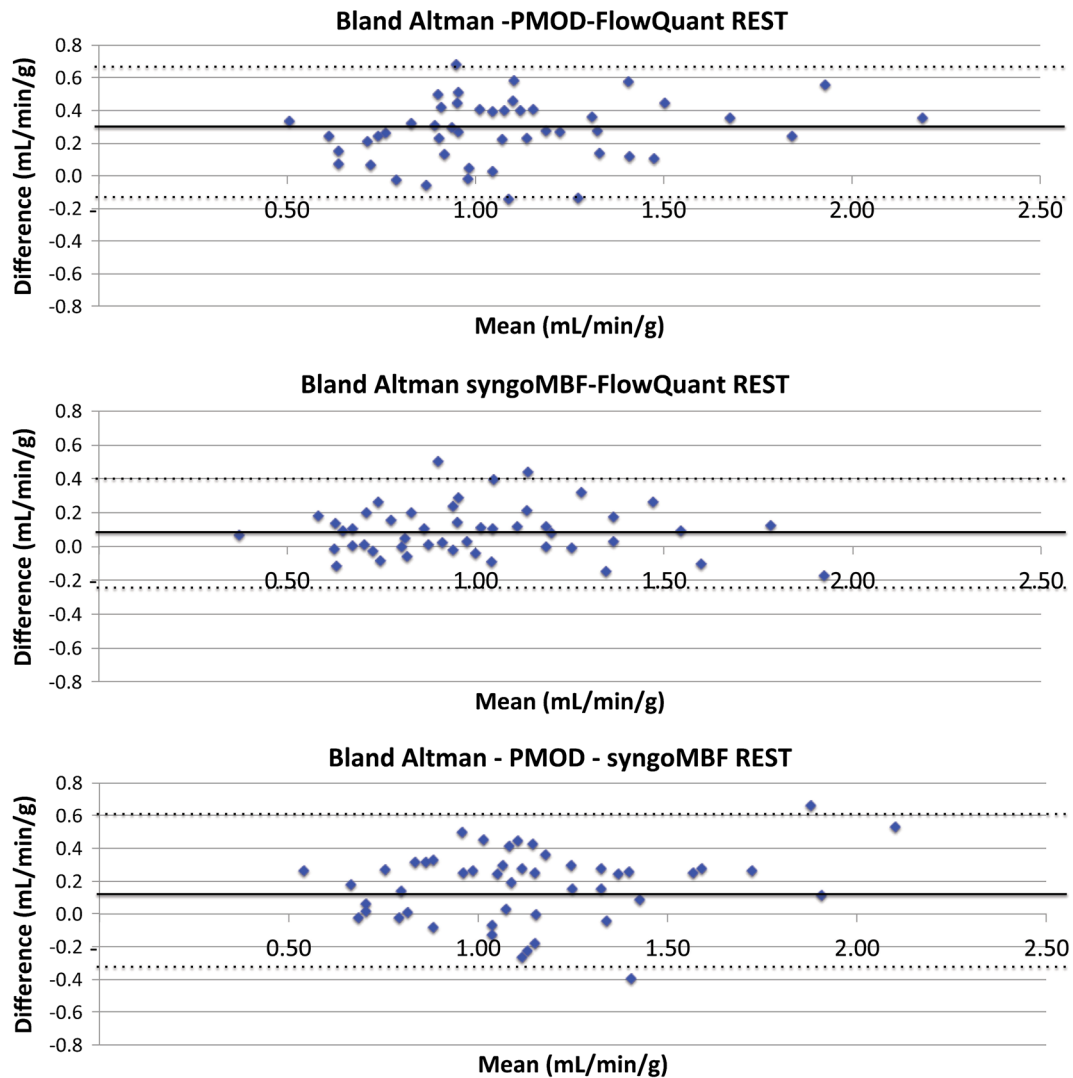


**Figure 3.** Bland-Altman plots illustrating differences in calculated rest myocardial blood flow three combinations of software. *Solid black line* is the mean difference, and *dotted black lines* are  $\pm 2$  standard deviations.

**Results by Myocardial Segments.** Resting blood flow in the three myocardial vascular territories demonstrated a wide range of flows from 0.28 to 2.3 mL·minute<sup>-1</sup>·g<sup>-1</sup> (FlowQuant), 0.40-2.1 mL·minute<sup>-1</sup>·g<sup>-1</sup> (syngo MBF), and 0.53-2.7 mL·minute<sup>-1</sup>·g<sup>-1</sup> (PMOD). Stress flows for individual myocardial segments had a predictably larger range from 0.68 to 4.5 mL·minute<sup>-1</sup>·g<sup>-1</sup> (FlowQuant), 0.85 to 4.7 mL·minute<sup>-1</sup>·g<sup>-1</sup> (syngo MBF), and 0.94 to 6.2 mL·minute<sup>-1</sup>·g<sup>-1</sup> (PMOD).

When all subject data was combined, and for combined male and combined female cohorts, mean flows to tissue fed by the RCA were always higher than

flows from the LCX (mean 17-27%, depending upon the software package). These differences were consistent under both rest and stress conditions, and significant at the  $P = .05$  level. The RCA also had uniformly higher flows than the LAD under both rest and stress conditions (mean 8%-19% higher depending upon the software package), however, these differences, despite their consistency, did not meet statistical significance. The LAD flows were generally, but not always, higher than LCX flows. A complete presentation of mean rest and stress MBF and MFR by segment for each of the software packages are listed in Table 1.

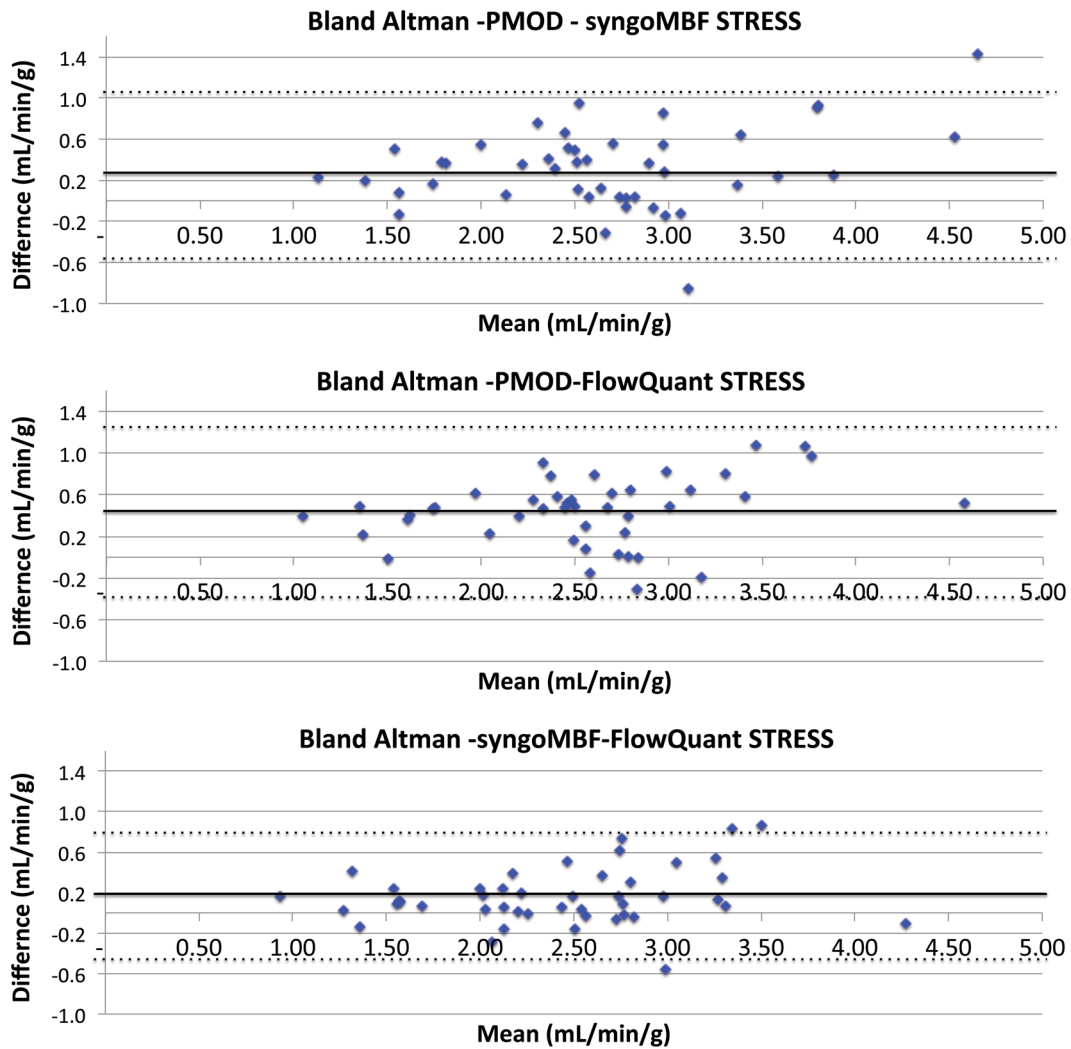


**Figure 4.** Bland-Altman plots illustrating differences in calculated stress myocardial blood flow three combinations of software. *Solid black line* is the mean difference, and *dotted black lines* are  $\pm 2$  standard deviations.

An example of the frequency distribution of MBF under resting conditions for the three vascular territories take from FlowQuant data is illustrated in Figure 7A. The other software packages showed similar distributions and trends. Figure 7B shows similar distribution across the vascular territories under stress conditions.

## DISCUSSION

Most early quantitative work with cardiovascularly normal subjects had small cohorts and was performed primarily to test and validate the methodology, and not necessarily generate normal MBF ranges. And of the few published investigations that did attempt to assess MBF variability in normal subject populations, conflicting results were reported. For example, some studies find no

MBF differences between male and female subjects,<sup>19</sup> while others do.<sup>18</sup> Some find differences in regional heterogeneity of MBF in vascular territories,<sup>18</sup> while others do not.<sup>11,19</sup> And some find general MBF and MFR trends with age,<sup>18</sup> while others find trends in opposite directions.<sup>19</sup> This work attempts to take a first step at untangling these multiple variables by systematically creating an age, sex, and vascular territory MBF and MFR normal database for Rb-82, the most commonly used clinical MBF tracer currently in use in the US.

In this study, we have generated the foundation for a quantitative normal Rb-82-based MBF database against which subsequent quantitative clinical Rb-82 perfusion scans can be compared. From these 49 cardiovascularly normal subjects, we tested three different software packages, each with the design capability to quantitate



**Table 1.** Tabulated normal database myocardial blood flow values ( $\text{mL}\cdot\text{minute}^{-1}\cdot\text{g}^{-1}$ ) and myocardial flow reserve by age, sex, and vascular territory for each of the three software packages

	PMOD LV		Syngo MBF		FlowQuant		PMOD LAD		syngo MBF		FlowQuant		PMOD RCA		syngo MBF		FlowQuant		PMOD LCX		syngo MBF		FlowQuant											
	stress	rest	LV stress	LV rest	FlowQuant	FlowQuant	stress	rest	LAD stress	LAD rest	FlowQuant	FlowQuant	stress	rest	RCA stress	RCA rest	FlowQuant	FlowQuant	stress	rest	RCA stress	RCA rest	FlowQuant	FlowQuant										
Female 40-49	2.91 ± 0.80	2.67 ± 0.5	2.40 ± 0.58	2.57 ± 0.93	2.43 ± 0.52	2.08 ± 0.65	3.58 ± 0.96	3.39 ± 1.02	2.94 ± 0.91	2.73 ± 0.82	2.89 ± 0.57	2.56 ± 0.60	2.51 ± 0.56	3.15 ± 0.67	2.92 ± 0.69	2.88 ± 0.74	2.86 ± 0.74	2.73 ± 0.71	2.93 ± 0.84	2.96 ± 0.50	2.36 ± 0.46	2.33 ± 0.81	2.19 ± 0.50	2.21 ± 0.63	2.10 ± 0.55	2.09 ± 0.56	1.97 ± 0.61	1.94 ± 0.57	2.03 ± 0.85	1.82 ± 0.68				
Female 50-59	3.09 ± 0.77	2.67 ± 0.71	2.52 ± 0.63	3.01 ± 0.81	2.61 ± 0.74	2.40 ± 0.61	3.39 ± 1.02	3.39 ± 1.02	2.94 ± 0.91	2.73 ± 0.82	2.89 ± 0.57	2.56 ± 0.60	2.51 ± 0.56	3.15 ± 0.67	2.92 ± 0.69	2.88 ± 0.74	2.86 ± 0.74	2.73 ± 0.71	2.93 ± 0.84	2.96 ± 0.50	2.36 ± 0.46	2.33 ± 0.81	2.19 ± 0.50	2.21 ± 0.63	2.10 ± 0.55	2.09 ± 0.56	1.97 ± 0.61	1.94 ± 0.57	2.03 ± 0.85	1.82 ± 0.68				
Female 60-69	3.20 ± 0.70	2.98 ± 0.70	2.73 ± 0.71	3.11 ± 0.82	2.98 ± 0.82	2.69 ± 0.75	3.51 ± 0.73	3.41 ± 2.36	2.93 ± 0.84	2.96 ± 0.50	2.36 ± 0.46	2.33 ± 0.81	2.19 ± 0.50	3.41 ± 2.36	2.93 ± 0.84	2.96 ± 0.50	2.36 ± 0.46	2.33 ± 0.81	2.19 ± 0.50	2.21 ± 0.63	2.10 ± 0.55	2.09 ± 0.56	1.97 ± 0.61	1.94 ± 0.57	2.03 ± 0.85	1.82 ± 0.68	2.03 ± 0.85	1.82 ± 0.68	2.03 ± 0.85	1.82 ± 0.68				
Male 40-49	2.99 ± 0.39	2.72 ± 0.80	2.53 ± 0.43	2.86 ± 0.51	2.84 ± 0.85	2.47 ± 0.45	2.71 ± 0.64	2.90 ± 1.42	2.49 ± 0.99	2.27 ± 0.85	2.27 ± 1.06	2.03 ± 0.85	1.82 ± 0.68	2.71 ± 0.64	2.49 ± 0.99	2.27 ± 0.85	2.27 ± 1.06	2.03 ± 0.85	1.82 ± 0.68	2.49 ± 0.99	2.27 ± 0.85	2.27 ± 1.06	2.03 ± 0.85	1.82 ± 0.68	2.49 ± 0.99	2.27 ± 0.85	2.27 ± 1.06	2.03 ± 0.85	1.82 ± 0.68	2.49 ± 0.99	2.27 ± 0.85	2.27 ± 1.06	2.03 ± 0.85	1.82 ± 0.68
Male 50-59	2.40 ± 0.50	2.16 ± 0.58	2.04 ± 0.53	2.40 ± 0.54	2.24 ± 0.67	2.05 ± 0.64	2.71 ± 0.64	2.90 ± 1.42	2.49 ± 0.99	2.27 ± 0.85	2.27 ± 1.06	2.03 ± 0.85	1.82 ± 0.68	2.71 ± 0.64	2.49 ± 0.99	2.27 ± 0.85	2.27 ± 1.06	2.03 ± 0.85	1.82 ± 0.68	2.49 ± 0.99	2.27 ± 0.85	2.27 ± 1.06	2.03 ± 0.85	1.82 ± 0.68	2.49 ± 0.99	2.27 ± 0.85	2.27 ± 1.06	2.03 ± 0.85	1.82 ± 0.68	2.49 ± 0.99	2.27 ± 0.85	2.27 ± 1.06	2.03 ± 0.85	1.82 ± 0.68
Male 60-69	2.61 ± 1.20	2.31 ± 0.87	2.07 ± 0.76	2.63 ± 1.16	2.38 ± 0.86	2.09 ± 0.77	2.90 ± 1.42	2.90 ± 1.42	2.49 ± 0.99	2.27 ± 0.85	2.27 ± 1.06	2.03 ± 0.85	1.82 ± 0.68	2.90 ± 1.42	2.49 ± 0.99	2.27 ± 0.85	2.27 ± 1.06	2.03 ± 0.85	1.82 ± 0.68	2.49 ± 0.99	2.27 ± 0.85	2.27 ± 1.06	2.03 ± 0.85	1.82 ± 0.68	2.49 ± 0.99	2.27 ± 0.85	2.27 ± 1.06	2.03 ± 0.85	1.82 ± 0.68	2.49 ± 0.99	2.27 ± 0.85	2.27 ± 1.06	2.03 ± 0.85	1.82 ± 0.68
	PMOD LV		syngo MBF		FlowQuant		PMOD LAD		syngo MBF		FlowQuant		PMOD RCA		syngo MBF		FlowQuant		PMOD LCX		syngo MBF		FlowQuant											
	rest	rest	LV rest	LV rest	LAD rest	LAD rest	rest	rest	LAD rest	LAD rest	rest	rest	rest	rest	RCA rest	RCA rest	rest	rest	rest	rest	RCA rest	RCA rest	rest	rest										
Female 40-49	1.46 ± 0.46	1.28 ± 0.44	1.25 ± 1.11	1.32 ± 0.39	1.19 ± 0.36	1.11 ± 0.28	1.69 ± 0.62	1.47 ± 0.59	1.49 ± 0.51	1.43 ± 0.44	1.27 ± 0.49	1.24 ± 0.48	1.47 ± 0.59	1.49 ± 0.51	1.43 ± 0.44	1.27 ± 0.49	1.24 ± 0.48	1.47 ± 0.59	1.49 ± 0.51	1.43 ± 0.44	1.27 ± 0.49	1.24 ± 0.48	1.47 ± 0.59	1.49 ± 0.51	1.43 ± 0.44	1.27 ± 0.49	1.24 ± 0.48	1.47 ± 0.59	1.49 ± 0.51	1.43 ± 0.44	1.27 ± 0.49	1.24 ± 0.48		
Female 50-59	1.47 ± 0.50	1.22 ± 0.38	1.12 ± 0.47	1.47 ± 0.60	1.22 ± 0.38	1.06 ± 0.52	1.58 ± 0.47	1.31 ± 0.40	1.24 ± 0.53	1.35 ± 0.47	1.17 ± 0.38	1.09 ± 0.42	1.31 ± 0.40	1.24 ± 0.53	1.35 ± 0.47	1.17 ± 0.38	1.09 ± 0.42	1.31 ± 0.40	1.24 ± 0.53	1.35 ± 0.47	1.17 ± 0.38	1.09 ± 0.42	1.31 ± 0.40	1.24 ± 0.53	1.35 ± 0.47	1.17 ± 0.38	1.09 ± 0.42	1.31 ± 0.40	1.24 ± 0.53	1.35 ± 0.47	1.17 ± 0.38	1.09 ± 0.42		
Female 60-69	1.11 ± 0.17	1.14 ± 0.24	0.91 ± 0.22	1.11 ± 0.18	1.17 ± 0.30	0.92 ± 0.24	1.18 ± 0.27	1.19 ± 0.27	0.94 ± 0.26	0.99 ± 0.16	1.07 ± 0.23	0.86 ± 0.18	1.19 ± 0.27	0.94 ± 0.26	0.99 ± 0.16	1.07 ± 0.23	0.86 ± 0.18	1.19 ± 0.27	0.94 ± 0.26	0.99 ± 0.16	1.07 ± 0.23	0.86 ± 0.18	1.19 ± 0.27	0.94 ± 0.26	0.99 ± 0.16	1.07 ± 0.23	0.86 ± 0.18	1.19 ± 0.27	0.94 ± 0.26	0.99 ± 0.16	1.07 ± 0.23	0.86 ± 0.18		
Male 40-49	1.16 ± 0.18	1.05 ± 0.20	0.90 ± 0.13	1.06 ± 0.25	1.05 ± 0.20	0.85 ± 0.21	1.32 ± 0.39	1.25 ± 0.16	1.11 ± 0.10	0.91 ± 0.18	0.86 ± 0.22	0.76 ± 0.22	1.25 ± 0.16	1.11 ± 0.10	0.91 ± 0.18	0.86 ± 0.22	0.76 ± 0.22	1.25 ± 0.16	1.11 ± 0.10	0.91 ± 0.18	0.86 ± 0.22	0.76 ± 0.22	1.25 ± 0.16	1.11 ± 0.10	0.91 ± 0.18	0.86 ± 0.22	0.76 ± 0.22	1.25 ± 0.16	1.11 ± 0.10	0.91 ± 0.18	0.86 ± 0.22	0.76 ± 0.22		
Male 50-59	1.22 ± 0.31	0.91 ± 0.32	0.90 ± 0.84	1.15 ± 0.31	0.91 ± 0.32	0.84 ± 0.28	1.53 ± 0.52	1.08 ± 0.52	1.10 ± 0.28	1.01 ± 0.27	0.82 ± 0.25	0.81 ± 0.30	1.08 ± 0.52	1.10 ± 0.28	1.01 ± 0.27	0.82 ± 0.25	0.81 ± 0.30	1.08 ± 0.52	1.10 ± 0.28	1.01 ± 0.27	0.82 ± 0.25	0.81 ± 0.30	1.08 ± 0.52	1.10 ± 0.28	1.01 ± 0.27	0.82 ± 0.25	0.81 ± 0.30	1.08 ± 0.52	1.10 ± 0.28	1.01 ± 0.27	0.82 ± 0.25	0.81 ± 0.30		
Male 60-69	1.00 ± 0.29	0.85 ± 0.21	0.76 ± 0.21	1.04 ± 0.32	0.85 ± 0.21	0.77 ± 0.23	1.08 ± 0.38	0.88 ± 0.26	0.87 ± 0.32	0.87 ± 0.28	0.73 ± 0.17	0.65 ± 0.17	0.88 ± 0.26	0.87 ± 0.32	0.87 ± 0.28	0.73 ± 0.17	0.65 ± 0.17	0.88 ± 0.26	0.87 ± 0.32	0.87 ± 0.28	0.73 ± 0.17	0.65 ± 0.17	0.88 ± 0.26	0.87 ± 0.32	0.87 ± 0.28	0.73 ± 0.17	0.65 ± 0.17	0.88 ± 0.26	0.87 ± 0.32	0.87 ± 0.28	0.73 ± 0.17	0.65 ± 0.17		
	PMOD LV		syngo MBF		FlowQuant		PMOD LAD		syngo MBF		FlowQuant		PMOD RCA		syngo MBF		FlowQuant		PMOD LCX		syngo MBF		FlowQuant											
	MFR	MFR	LV MFR	LV MFR	LAD MFR	LAD MFR	MFR	MFR	LAD MFR	LAD MFR	MFR	MFR	MFR	MFR	RCA MFR	RCA MFR	MFR	MFR	MFR	MFR	RCA MFR	RCA MFR	MFR	MFR										
Female 40-49	2.10 ± 0.60	2.28 ± 0.63	2.03 ± 0.46	1.99 ± 0.52	2.17 ± 0.49	1.91 ± 0.36	2.30 ± 0.82	2.55 ± 1.02	2.17 ± 0.62	2.00 ± 0.55	2.22 ± 0.64	2.11 ± 0.55	2.55 ± 1.02	2.17 ± 0.62	2.00 ± 0.55	2.22 ± 0.64	2.11 ± 0.55	2.55 ± 1.02	2.17 ± 0.62	2.00 ± 0.55	2.22 ± 0.64	2.11 ± 0.55	2.55 ± 1.02	2.17 ± 0.62	2.00 ± 0.55	2.22 ± 0.64	2.11 ± 0.55	2.55 ± 1.02	2.17 ± 0.62	2.00 ± 0.55	2.22 ± 0.64	2.11 ± 0.55		
Female 50-59	2.23 ± 0.76	2.51 ± 0.79	2.62 ± 1.12	2.21 ± 0.82	2.37 ± 0.77	2.62 ± 1.12	2.25 ± 0.77	2.38 ± 0.75	2.56 ± 1.17	2.26 ± 0.75	2.47 ± 0.76	2.66 ± 1.23	2.38 ± 0.75	2.56 ± 1.17	2.26 ± 0.75	2.47 ± 0.76	2.66 ± 1.23	2.38 ± 0.75	2.56 ± 1.17	2.26 ± 0.75	2.47 ± 0.76	2.66 ± 1.23	2.38 ± 0.75	2.56 ± 1.17	2.26 ± 0.75	2.47 ± 0.76	2.66 ± 1.23	2.38 ± 0.75	2.56 ± 1.17	2.26 ± 0.75	2.47 ± 0.76	2.66 ± 1.23		
Female 60-69	2.94 ± 0.75	2.71 ± 0.58	3.14 ± 0.64	2.88 ± 0.81	2.64 ± 0.66	3.04 ± 0.79	3.08 ± 0.89	2.75 ± 0.68	3.21 ± 0.62	2.94 ± 0.71	2.77 ± 0.61	3.23 ± 0.58	2.75 ± 0.68	3.21 ± 0.62	2.94 ± 0.71	2.77 ± 0.61	3.23 ± 0.58	2.75 ± 0.68	3.21 ± 0.62	2.94 ± 0.71	2.77 ± 0.61	3.23 ± 0.58	2.75 ± 0.68	3.21 ± 0.62	2.94 ± 0.71	2.77 ± 0.61	3.23 ± 0.58	2.75 ± 0.68	3.21 ± 0.62	2.94 ± 0.71	2.77 ± 0.61	3.23 ± 0.58		
Male 40-49	2.64 ± 0.55	2.67 ± 0.60	3.00 ± 0.44	2.77 ± 0.46	2.74 ± 0.57	3.08 ± 0.66	2.69 ± 0.68	2.37 ± 0.65	2.71 ± 0.31	2.67 ± 0.67	2.83 ± 0.84	3.16 ± 1.11	2.37 ± 0.65	2.71 ± 0.31	2.67 ± 0.67	2.83 ± 0.84	3.16 ± 1.11	2.37 ± 0.65	2.71 ± 0.31	2.67 ± 0.67	2.83 ± 0.84	3.16 ± 1.11	2.37 ± 0.65	2.71 ± 0.31	2.67 ± 0.67	2.83 ± 0.84	3.16 ± 1.11	2.37 ± 0.65	2.71 ± 0.31	2.67 ± 0.67	2.83 ± 0.84	3.16 ± 1.11		
Male 50-59	2.12 ± 0.82	2.85 ± 1.45	2.85 ± 1.68	2.31 ± 1.16	3.06 ± 1.85	3.02 ± 1.97	2.03 ± 1.04	2.49 ± 1.20	2.31 ± 1.13	2.22 ± 0.87	2.80 ± 1.38	3.09 ± 2.05	2.49 ± 1.20	2.31 ± 1.13	2.22 ± 0.87	2.80 ± 1.38	3.09 ± 2.05	2.49 ± 1.20	2.31 ± 1.13	2.22 ± 0.87	2.80 ± 1.38	3.09 ± 2.05	2.49 ± 1.20	2.31 ± 1.13	2.22 ± 0.87	2.80 ± 1.38	3.09 ± 2.05	2.49 ± 1.20	2.31 ± 1.13	2.22 ± 0.87	2.80 ± 1.38	3.09 ± 2.05		
Male 60-69	2.83 ± 1.63	2.95 ± 1.21	3.01 ± 1.29	2.80 ± 1.50	2.93 ± 1.08	3.01 ± 1.18	3.03 ± 2.08	3.01 ± 1.58	2.97 ± 1.37	2.80 ± 1.47	2.91 ± 1.23	3.16 ± 1.50	3.01 ± 1.58	2.97 ± 1.37	2.80 ± 1.47	2.91 ± 1.23	3.16 ± 1.50	3.01 ± 1.58	2.97 ± 1.37	2.80 ± 1.47	2.91 ± 1.23	3.16 ± 1.50	3.01 ± 1.58	2.97 ± 1.37	2.80 ± 1.47	2.91 ± 1.23	3.16 ± 1.50	3.01 ± 1.58	2.97 ± 1.37	2.80 ± 1.47	2.91 ± 1.23	3.16 ± 1.50		

All values are mean ± 1 standard deviation.

MFR, Myocardial flow reserve; LV, left ventricle; RCA, right coronary artery; LAD, left anterior descending artery; LCX, left circumflex artery.

**Table 2.** Tabulated normal database myocardial blood flow values ( $\text{mL} \cdot \text{minute}^{-1} \cdot \text{g}^{-1}$ ) and myocardial flow reserve, all ages combined, by sex and vascular territory for each of the three software packages

	PMOD LV stress	syngo MBF LV stress	FlowQuant LV stress	PMOD LAD stress	syngo MBF LAD stress	FlowQuant LAD stress	PMOD RCA stress	syngo MBF RCA stress	FlowQuant RCA stress	PMOD LCX stress	syngo MBF LCX stress	FlowQuant LCX stress
Female (All)	3.10 ± 0.72	2.80 ± 0.66	2.60 ± 0.63	2.96 ± 0.83	2.73 ± 0.74	2.45 ± 0.69	3.48 ± 0.86	3.10 ± 0.74	2.87 ± 0.72	2.85 ± 0.63	2.68 ± 0.64	2.57 ± 0.61
Male (all)	2.60 ± 0.84	2.33 ± 0.75	2.15 ± 0.62	2.58 ± 0.83	2.42 ± 0.78	2.15 ± 0.66	2.92 ± 1.03	2.47 ± 0.84	2.34 ± 0.73	2.21 ± 0.76	2.06 ± 0.73	1.94 ± 0.60
	PMOD LV rest	syngo MBF LV rest	FlowQuant LV rest	PMOD LAD rest	syngo MBF LAD rest	FlowQuant LAD rest	PMOD RCA rest	syngo MBF RCA rest	FlowQuant RCA rest	PMOD LCX rest	syngo MBF LCX rest	FlowQuant LCX rest
Female (All)	1.32 ± 0.42	1.20 ± 0.33	1.06 ± 0.38	1.30 ± 0.45	1.19 ± 0.35	1.01 ± 0.38	1.44 ± 0.47	1.29 ± 0.39	1.17 ± 0.47	1.22 ± 0.40	1.15 ± 0.34	1.03 ± 0.37
Male (all)	1.12 ± 0.29	0.90 ± 0.26	0.85 ± 0.24	1.09 ± 0.30	0.91 ± 0.26	0.81 ± 0.24	1.31 ± 0.47	1.03 ± 0.39	1.01 ± 0.38	0.93 ± 0.26	0.79 ± 0.21	0.74 ± 0.24
	PMOD LV MFR	syngo MBF LV MFR	FlowQuant LV MFR	PMOD LAD MFR	syngo MBF LAD MFR	FlowQuant LAD MFR	PMOD RCA MFR	syngo MBF RCA MFR	FlowQuant RCA MFR	PMOD LCX MFR	syngo MBF LCX MFR	FlowQuant LCX MFR
Female (All)	2.50 ± 0.80	2.53 ± 0.67	2.71 ± 0.90	2.45 ± 0.83	2.44 ± 0.67	2.65 ± 0.94	2.61 ± 0.90	2.57 ± 0.77	2.75 ± 0.94	2.49 ± 0.78	2.54 ± 0.68	2.78 ± 0.95
Male (All)	2.50 ± 1.19	2.85 ± 1.19	2.94 ± 1.31	2.51 ± 1.19	2.94 ± 1.34	3.03 ± 1.43	2.56 ± 1.52	2.67 ± 1.28	2.65 ± 1.14	2.54 ± 1.11	2.85 ± 1.18	3.13 ± 1.62

All values are mean ± 1 standard deviation.

MFR, Myocardial flow reserve; LV, left ventricle; RCA, right coronary artery; LAD, left anterior descending artery; LCX, left circumflex artery.

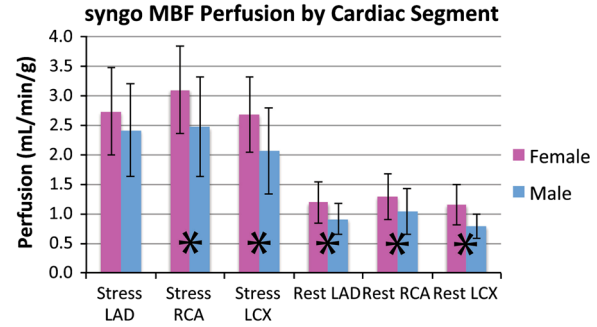


**Figure 5.** Sample myocardial perfusion results for males and females as calculated by syngo MBF. Differences between mean flow values for females and males achieved statistical significance at the 0.05 level (\*) for all cardiac vascular territories except the LAD under stress conditions. Other software packages demonstrated similar significant differences between the sexes.

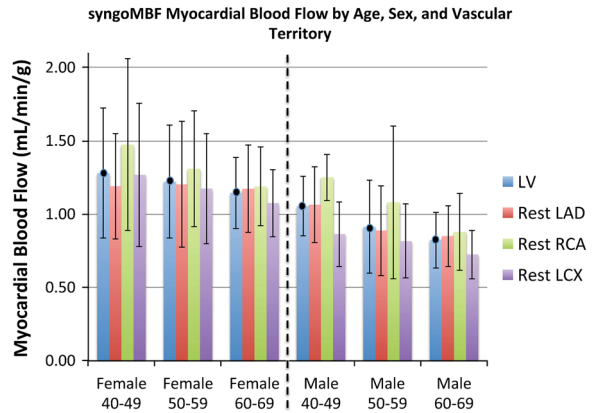


**Figure 6.** Resting myocardial blood flow, as calculated by syngo MBF by age, sex, and vascular territory. There is a tendency toward decreasing flow with age evident in both males and females.

Rb-82 MBF using a single compartment model, and from those measurements also generated MFR data. The primary purposes were to (1) assess the degree of concurrence between these software packages, and to collect and generate normal MBF and MFR database values for data generated from each and (2) to categorize and analyze the MBF and MFR data by sex, age, and myocardial vascular territory for purposes of understanding quantitative trends and subdividing categories in the database to facilitate comparisons with like populations.

The software comparison results can be summarized as follows. (1) All three software programs tested generated physiologically meaningful quantitative MBF and MFR values in all patients that are consistent with previously reported measurement ranges. (2) Differences in MBF measurements under both rest and stress conditions, for both males and female, on the order of 20%, were observed between PMOD and FlowQuant

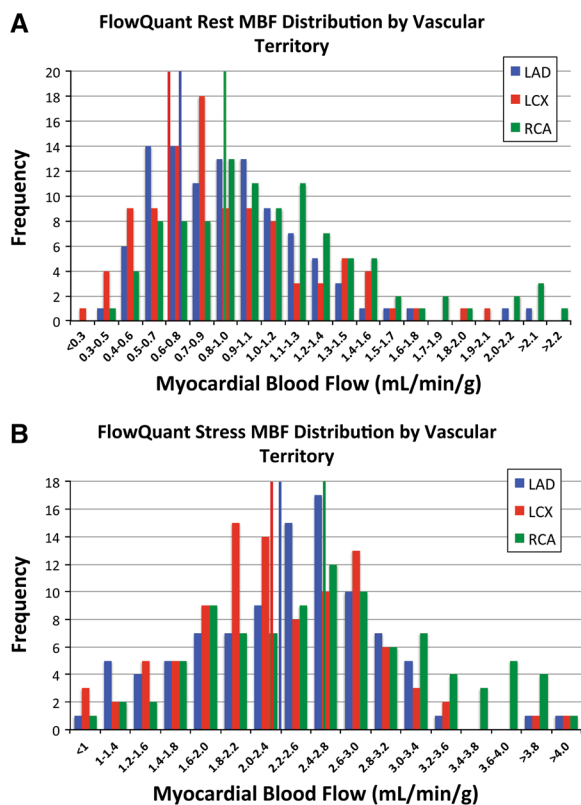


**Figure 7.** (A) FlowQuant-based frequency distribution of resting MBF for LAD, mean =  $0.91 \text{ mL} \cdot \text{minute}^{-1} \cdot \text{g}^{-1}$ ; LCX, mean =  $0.88 \text{ mL} \cdot \text{minute}^{-1} \cdot \text{g}^{-1}$ ; and RCA, mean =  $1.09 \text{ mL} \cdot \text{minute}^{-1} \cdot \text{g}^{-1}$ . Rest means are graphically represented by full length vertical lines (green for RCA, blue for LAD, and red for LCX). PMOD and syngo MBF had similar distributions with mean MBFs  $\text{RCA} > \text{LAD} > \text{LCX}$ . (B) Analogous frequency distribution for stress MBF shows a similar relative distribution. Note that histogram ranges on the x-axis for both plots use overlapping ranges so as to smooth the distribution and make the relative shapes of the curves more apparent.

(PMOD > FlowQuant). These differences were significant at the  $P = .05$  level. Smaller MBF value differences between PMOD and syngo MBF were observed, on the order of 12%, but statistical significance of these differences was less compelling. syngo MBF demonstrated a nominal 9% positive bias when compared to FlowQuant, and did not approach significant difference. There were no discernible differences or software biases relative to the MFR measurements. Presumably the individual software-associated MFR biases for both stress and rest measurements cancel one another out in the MFR ratio calculation.

The MBF and MFR measurements, grouped into sex, age, and myocardial vascular territory categories, result in the following summary observations: (1) Female MBF is statistically higher (about 20%) than corresponding male MBF under both rest and pharmacological stress conditions. This relationship held both globally and relative to

individual vascular territories. (2) For the age range studied, 40-69, MBF generally decreased with age. (3) Global MFR values demonstrated a weakly increasing trend with age with no significant MFR trends related to gender discernable. (4) The tissue fed by the RCA was consistently the most highly perfused region of the myocardium, on the order of 20% and 10% higher than tissue fed by the LCX and LAD, respectively. This distribution held almost universally for individual subjects as well as the population at large.

The quantitative findings presented in this work are generally, but not completely, concordant with values and patterns of other quantitative blood flow studies of normal populations. Many of these earlier studies were performed in an earlier phase of PET technology development, and were performed to better understand the magnitude and patterns of pharmacologically induced hyperemia, technological test-retest quantitative reproducibility, and identification of the impact of age, sex, and regional heterogeneity.<sup>12,18,19</sup> The primary purpose of this study was more translational in focus, attempting to confirm previous cardiovascularly normal population findings using current generation commercial software, and to generate a normal database as a tool and reference for subsequent clinical use.

The largest normal study in the literature was published in 2000, used  $[^{15}\text{O}]\text{H}_2\text{O}$  as the flow agent, and was retrospectively compiled MBF and MFR data from 169 cardiovascularly normal subjects who were involved in  $[^{15}\text{O}]\text{H}_2\text{O}$  blood flow research projects that required normal cardiac vasculature.<sup>18</sup> Our resting flows mesh well with these reported results, however, our Rb-82-based dipyridamole hyperemia measurements appear lower than the reported values ( $2.6\text{-}3.1 \text{ mL} \cdot \text{minute}^{-1} \cdot \text{g}^{-1}$  for our study, depending upon the software vs  $3\text{-}4 \text{ mL} \cdot \text{minute}^{-1} \cdot \text{g}^{-1}$  for the Chareonthaitawee report).<sup>18</sup> The differential in hyperemic flow results in marginally lower comparison MFR values.

Regional heterogeneity analysis of MBF generated interesting results. Our study observed statistically significant differences of MBF from the RCA relative to other parts of the myocardium. This flow pattern was not identified in any  $[^{15}\text{O}]\text{H}_2\text{O}$  or  $[^{13}\text{N}]\text{ammonia}$  studies. However, the relative MBF distribution pattern was reported in another Rb-82 study with a normal population.<sup>11</sup> Of particular import in this related work was that it was a comparator study with  $[^{13}\text{N}]\text{ammonia}$ , and this particular anatomic uptake was not observed, suggesting a tracer-specific regional uptake phenomenon.

Since statistically significant differences were found between males and females, with age, and by vascular territory, the need for a reliable age and sex-matched normal database is becoming increasingly apparent. These differences are apparent even with the relatively

small number of normal subjects per each category suggesting that a database even with modest representation per category might be useful.

With regard to software-based differences, both the mean MBF differences between populations, and individual differences in MBF were the focus of follow-up investigation. Investigating sources of these differences was deemed of particular importance because the presented work demonstrated a bias between syngo MBF and FlowQuant that was not observed in previous published work.<sup>20</sup> Attempts were made to identify the core sources of these differences. Since each software package had its own unique blood VOI definition approach, it was an obvious source of potential bias. We identified those studies where blood input function were discordant (peak height, shape, area under the blood curve) between software packages and investigated whether these same patients had discordant MBF values. However, no correlation between discordant input functions and discordant MBF were found. We additionally investigated whether when global myocardial flow differences for an individual patient were associated with a systematic myocardial segment that was either being under or overestimated, biasing the global result. This would particularly make sense in regions like the septa, where PMOD uses a right ventricular spillover correction, and the other software does not. However upon analysis, the differences tended to be global rather than driven by specific segments.

Three patients showed lack of significant increase flow due to dipyridamole as evidenced by MFR close to unity (subjects 8, 31, and 32 in Figure 2). Caffeine, an adenosine antagonist, is potential cause. No-caffeine compliance was verbally verified prior to study commencement, but there was no pharmacologic verification, so non-compliance could have been a factor in these results. Since there was no reason to exclude this data, it was included in all tabulated results.

We measured and observed a broad range of rest and stress MBF in our normal population. This wide, naturally occurring variability has been reported in the literature. It was our hope that accounting for age and sex would substantially decrease the range of normal variability adding additional significant clinical value to the measurement. Breaking down normal subject populations into age and sex-matched cohorts was found to decrease the variance of normal MBF and MFR when compared to the entire group of 49 normal subjects, however, even after subcategorizing the populations the range of normal measurements remained large. This confirmed reality places limits the utility of comparing individual patient data against even age and sex-matched normal MBF and MFR. As this range of normal flows appears both real and innate, it would be difficult to imagine strategies to further minimize these variabilities. It is recognized that based upon the results of

this study, it would be difficult to definitively classify quantitative MBF measurements as normal or abnormal when using the quantitatively derived PET MBF values as the only criteria, devoid of other clinical data.

However, cardiac PET scans are performed for a clinical purpose and are interpreted in clinical context; in many cases quantitative MBF and MFR can provide additional clinically meaningful information. Examples include quantitative assessing the impact of treatment via pre- and post-MBF assessment, putting into context the perfusion implications of multi-vessel disease, and assessment of the physiologic importance of a known stenosis to guide treatment. The latter situation can be addressed because the myocardial segments in individual normal subjects proved remarkably consistent within individuals. Quantitative assessment of smaller focal decreases in the MBF polar maps can not only be quantitated in absolute terms, but to grade the perfusion impact of a known stenosis. In all these situations, knowledge of intra and inter-subject variability in normal populations plays an important role.

## NEW KNOWLEDGE GAINED

MBF as measured by quantitative Rb-82 PET demonstrates statistically significant dependency on age and gender. With Rb-82-based measurements, the vascular territory fed by the RCA had higher flows than the LAD, which were higher than the LCX, which may be a radiopharmaceutical specific distribution because the pattern has not been observed in [<sup>15</sup>O]H<sub>2</sub>O or [<sup>13</sup>N]ammonia studies. Even when using the same pharmacokinetic model with identical fundamental modeling assumptions, different software generates statistically significant MBF and MFR values. MFR, a potentially clinically valuable quantitative metric, was less sensitive to sex, age, myocardial distribution, and software than MBF.

## CONCLUSION

The current version of the quantitative Rb-82 normal database consisting of 49 subjects resulted in several statistically significant conclusions that support the need for a software specific, radiopharmaceutical specific, age, and sex-matched database to aid in interpretation of quantitative clinical myocardial perfusion studies.

## Disclosure

*First Author (Sunderland) received research funding from Siemens Medical Solutions for the performance of the research presented. Drs. Pan and Declerck are employees of Siemens Molecular Imaging, the IP holders for one of the pieces of software tested and presented. Dr. Pan was involved in early*

*processing of the data for syngo MBF in earlier software versions and provided technical modeling support. Both Drs. Pan and Declerck were involved in editing the manuscript.*

## References

- Goldstein RA. Rubidium-82 kinetics after coronary occlusion: Temporal relation of net myocardial accumulation and viability in open-chested dogs. *J Nucl Med* 1986;27(9):1456-61.
- Herrero P, Markham J, Shelton ME, Weinheimer CJ, Bergmann SR. Noninvasive quantification of regional myocardial perfusion with rubidium-82 and positron emission tomography. Exploration of a mathematical model. *Circulation* 1990;82(4):1377-86.
- Huang SC, Williams BA, Williams BA, Krivokapich J, Araujo L, Araujo L, et al. Rabbit myocardial <sup>82</sup>Rb kinetics and a compartmental model for blood flow estimation. *Am J Physiol* 1989;256(4 Pt 2):H1156-64.
- Krivokapich J, Smith GT, Huang SC, Hoffman EJ, Ratib O, Phelps ME, et al. <sup>13</sup>N ammonia myocardial imaging at rest and with exercise in normal volunteers. Quantification of absolute myocardial perfusion with dynamic positron emission tomography. *Circulation* 1989;80(5):1328-37.
- Yoshida K, Yoshida K, Mullani N, Mullani N, Gould KL. Coronary flow and flow reserve by PET simplified for clinical applications using rubidium-82 or nitrogen-13-ammonia. *J Nucl Med* 1996;37(10):1701-12.
- Ziadi MC, Beanlands RSB. The clinical utility of assessing myocardial blood flow using positron emission tomography. *J Nucl Cardiol* 2010;17(4):571-81.
- Klein R, Beanlands RSB, deKemp RA. Quantification of myocardial blood flow and flow reserve: Technical aspects. *J Nucl Cardiol* 2010;17(4):555-70.
- Lortie M, Beanlands R, Yoshinaga K, Klein R. Quantification of myocardial blood flow with <sup>82</sup>Rb dynamic PET imaging. *Eur J Med Mol Imaging* 2007;34:1765-74.
- Wisenberg G, Schelbert HR, Hoffman EJ, Phelps ME, Robinson GD Jr, Selin CE, et al. In vivo quantitation of regional myocardial blood flow by positron-emission computed tomography. *Circulation* 1981;63(6):1248-58.
- Nakazato R, Berman DS, Dey D, Le Meunier L, Hayes SW, Fermin JS, et al. Automated quantitative Rb-82 3D PET/CT myocardial perfusion imaging: Normal limits and correlation with invasive coronary angiography. *J Nucl Cardiol* 2012;19(2):265-76.
- El Fakhri G, Kardan A, Sitek A, Dorbala S. Reproducibility and accuracy of quantitative myocardial blood flow assessment with <sup>82</sup>Rb PET: Comparison with <sup>13</sup>N-ammonia PET. *J Nucl Med* 2009;50:1062-71.
- Kaufmann PA, Gnecci-Ruscone T. Assessment of the reproducibility of baseline and hyperemic myocardial blood flow measurements with <sup>15</sup>O-labeled water and PET. *J Nucl Med* 1999;40:1848-56.
- Knešaurek K, Machac J, Zhang Z. Repeatability of regional myocardial blood flow calculation in <sup>82</sup>Rb PET imaging. *BMC Med Phys* 2009;9(1):2.
- Manabe O, Yoshinaga K, Katoh C, Naya M, deKemp RA, Tamaki N. Repeatability of rest and hyperemic myocardial blood flow measurements with <sup>82</sup>Rb dynamic PET. *J Nucl Med* 2008;50(1):68-71.
- Prior JO, Allenbach G, Valenta I, Kosinski M, Burger C, Verdun FR, et al. Quantification of myocardial blood flow with <sup>82</sup>Rb positron emission tomography: Clinical validation with <sup>15</sup>O-water. *Eur J Nucl Med Mol Imaging* 2012;39(6):1037-47.
- Renaud JM, Lortie M, DaSilva J. Quantification of the normal range of myocardial blood flow and flow reserve with <sup>82</sup>-rubidium versus <sup>13</sup>-N-ammonia PET. *IEEE Nucl Sci Symp Conf Rec* 2007;2007:3141-5.
- Beanlands RSB, Ziadi MC, Williams K. Quantification of myocardial flow reserve using positron emission imaging. *J Clin Use* 2009;54(2):157-9.
- Chareonthaitawee P, Kaufmann PA, Rimoldi O, Camici PG. Heterogeneity of resting and hyperemic myocardial blood flow in healthy humans. *Cardiovasc Res* 2001;50(1):151-61.
- Czernin J, Muller P, Chan S, Brunken RC, Porenta G, Krivokapich J, et al. Influence of age and hemodynamics on myocardial blood flow and flow reserve. *Circulation* 1993;88(1):62-9.
- Dekemp RA, Declerck J, Klein R, Pan X-B, Nakazato R, Tonge C, et al. Multisoftware reproducibility study of stress and rest myocardial blood flow assessed with 3D dynamic PET/CT and a 1-tissue-compartment model of <sup>82</sup>Rb kinetics. *J Nucl Med* 2013;54(4):571-7.
- Rajaram M, Tahari AK, Lee AH, Lodge MA, Tsui B, Nekolla S, et al. Cardiac PET/CT misregistration causes significant changes in estimated myocardial blood flow. *J Nucl Med* 2013;54(1):50-4.
- Esteves FP, Nye JA, Khan A, Folks RD, Halkar RK, Garcia EV, et al. Prompt-gamma compensation in Rb-82 myocardial perfusion 3D PET/CT. *J Nucl Cardiol* 2010;17(2):247-53.
- Martin CC, Christian BT, Satter MR, Nickerson LDH, Nickles RJ. Quantitative PET with positron emitters that emit prompt gamma rays. *IEEE Trans Med Imaging* 1995;14(4):681-7.
- Fukushima K, Javadi MS, Higuchi T, Lautamaki R, Merrill J, Nekolla SG, et al. Prediction of short-term cardiovascular events using quantification of global myocardial flow reserve in patients referred for clinical <sup>82</sup>Rb PET perfusion imaging. *J Nucl Med* 2011;52(5):726-32.
- Tio RA, Dabeshlim A, Siebelink HJM, de Sutter J, Hillege HL, Zeebregts CJ, et al. Comparison between the prognostic value of left ventricular function and myocardial perfusion reserve in patients with ischemic heart disease. *J Nucl Med* 2009;50(2):214-9.
- Fiechter M, Gebhard C, Ghadri JR, Fuchs TA, Pazhenkottil AP, Nkoulou RN, et al. Myocardial perfusion imaging with <sup>13</sup>N-ammonia PET is a strong predictor for outcome. *Int J Cardiol* 2013;167(3):1023-6.
- Ziadi MC, Dekemp RA, Williams KA, Guo A, Chow BJW, Renaud JM, et al. Impaired myocardial flow reserve on rubidium-82 positron emission tomography imaging predicts adverse outcomes in patients assessed for myocardial ischemia. *J Am Coll Cardiol* 2011;58(7):740-8.
- Saraste A, Kajander S, Han C, Nesterov SV, Knuuti J. PET: Is myocardial flow quantification a clinical reality? *J Nucl Cardiol* 2012;19(5):1044-59.
- Diamond GA, Forrester JS. Analysis of probability as an aid in the clinical diagnosis of coronary-artery disease. *N Engl J Med* 1979;300(24):1350-8.
- Pan X, Schindler T, Ratib O, Nekolla S, Declerck J. Effect of reorientation on myocardial blood flow estimation from dynamic <sup>13</sup>NH<sub>3</sub>PET imaging. In: 2009 IEEE Nuclear Science Symposium Conference Record (NSS/MIC). Orlando: IEEE; 2009.
- Pan X, Declerck J. White paper: Validation syngo.PET myocardial blood flow. Hoffman Estates: Siemens Medical Solutions; 2011. p. 1-17.
- Klein R, Renaud JM, Ziadi MC, Thorn SL, Adler A, Beanlands RS, et al. Intra- and inter-operator repeatability of myocardial blood flow and myocardial flow reserve measurements using rubidium-82 PET and a highly automated analysis program. *J Nucl Cardiol* 2010;17(4):600-16.